

SCIENTIFIC REPORTS



Trilocular phenotype in L. resulted from interruption of *CLAVATA1* gene homologue (*BjMc1*) transcription

Ping Xu¹, Shiqin Cao¹, Kaining Hu¹, Xiaohua Wang¹, Wei Huang¹

and *scd1*, showed the phenotype of multilocular siliques due to the disturbance of stem cell growth balance^{17, 18}. The *scd1* mutant showed multiloculus, and *scd1* was found to be required for the normal accumulation of various miRNAs, indicating that miRNAs might be involved in the regulation of silique trait¹⁹. In addition, a recent study showed that another receptor kinase signaling pathway involving *WIPK* regulated the stem cell growth, and the *wipk* mutant exhibited a similar silique trait with *scd1* mutants²⁰. In tomato, the mutation of the homologues of both *WIPK* and *IPK1* resulted in the increased number of fruit locules. Moreover, the mutation of the homologous genes in *WIPK* signaling pathway in maize^{21, 22} and rice²³, such as *WIPK* and *IPK1*, could also increase the seed number per inflorescence, which was similar to multilocular trait in rapeseed.

As a member of *WIPK* signaling pathway that regulates *WIPK* expression, more than 10 alleles of *WIPK* with multiloculus have been discovered in *Brassica napus*, and the mutants exhibited weak, intermediate and strong multilocular phenotypes^{12, 24, 25}. The *WIPK* gene encoded a putative receptor kinase²⁶, and mutation at different sites in the gene sequence could lead to different degrees of multilocular phenotype. Moreover, all the *WIPK* mutants with intermediate and strong multilocular phenotypes were dominant negative, and the mutant of *WIPK* homologous gene in tomato was also expected to be dominant-negative^{16, 27}. Similarly, most of the mutants with multiloculus discovered in *Brassica napus* showed variable valve numbers^{10, 11}. However, it has been unknown whether the molecular mechanism controlling multiloculus is similar between *Brassica napus* and *Brassica napus* or the dominant-negative character is associated with the instability of multilocular silique trait.

In previous study, we found that the trilobular silique always had three locules, and the trilobular plants had significantly higher yield per plant than the bilobular plants². The trilobular trait of *Brassica napus* was controlled by two independent recessive nuclear genes, *trilobular1* and *trilobular2*. The *trilobular1* and *trilobular2* gene were isolated from the same plants and mapped by molecular markers^{28, 29}. In present study, we cloned the bilobular gene *trilobular1* and trilobular *trilobular2* respectively. A Copia-LTR retrotransposable element 1 (RTE1) inserted in the coding region of *trilobular1* was identified in trilobular plants, which interrupted the transcription of the target gene. We also found that two amino acid sites had undergone positive selection in the ancestor of *Brassica napus* genes, and purifying selection was the dominant force after divergence of dicots and monocots from their common ancestor in the evolutionary process of *Brassica napus* genes, indicating that they were conserved in modern land plants.

Results

Fine mapping of *BjMc1* gene.

The *BjMc1* gene was previously mapped to a genomic region between marker EC14MC14 and SC20, which could delimit an interval of 2.7 cM²⁸. Compared with the bilobular siliques in NILs of *trilobular1* gene, the trilobular siliques displayed shorter, wider and flatter (Supplementary Fig. 1a,b). But the inflorescence meristem and floral meristem did not show differences between bilobular and trilobular plants in BC₆F₁ generation (Supplementary Fig. 2a,b). To identify the *BjMc1* gene locus, we further screened a BAC library of purple-leaf mustard with the primer C1-1 (Supplementary Table 1). Two positive clones, 26P20 and 83D02, were identified, and four scaffolds (designated as scaffold 1, 2, 3 and 4) (Supplementary Data 1) were obtained by sequencing 83D02. Two sequence-characterized amplified region markers SC40 and SC151 (Supplementary Table 1) were identified according to scaffold 2, and one SSR marker SR52 was identified based on scaffold 4. Subsequently, polymorphic markers SC40, SC151 and SR52 were used to search for the recombinants identifiable between SC13 and SC20. Among the 242 recombinants discovered from the NILs population which consisted of 9,300 individuals, 0, 4 and 8 recombination events were detected for SC40, SC151 and SR52 respectively. Finally, the candidate region of *BjMc1* was found to be restricted between SC151 and EC14MC14 at a 1.14-cM region. Twenty-five open reading frames (ORFs) of scaffold 2 in which both the co-segregative SC40 and nearest marker SC151 located were predicted according to: (<http://linux1.soe.berkeley.com/berky.phnml?topic=f>)

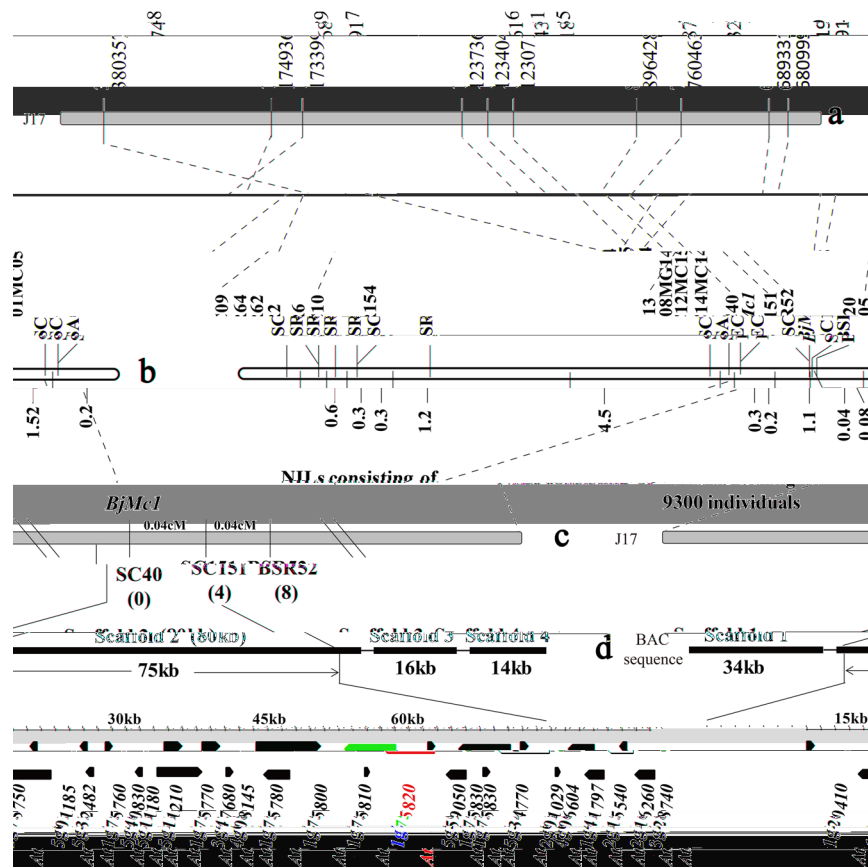


Fig. 1. Map-based cloning of the *Bjmc1* locus. (a) The physical location of molecular markers of the *Bjmc1* locus on J17 chromosome. (b) The genetic linkage map of the *Bjmc1* locus. (c) Genetic map showing the distance of the three markers identified in this research. (d) The scaffolds of BAC clone 83D02. The number below the marker indicates the number of recombinants between individual markers and the *Bjmc1* locus. The pentagons represent the predicted genes in the 75-kb target region on chromosome J17 of *B. juncea*. The candidate gene of *Bjmc1* is indicated by red color.

lines with *Bjmc1* (TGP1-4), 11 transgenic lines with *Bjmc1* (TGP5-15), and the bilocular and trilocular plants of BC₅F₁ generation were detected by qPCR using the primer DL2. As expected, compared with the bilocular plants of BC₅F₁ generation, the *Bjmc1*-transgenic plants showed much higher expression level of *Bjmc1*, while the *Bjmc1*-transgenic plants exhibited similar or lower expression level (Supplementary Fig. 3a).

In addition, the constructs of *Bjmc1* and *Bjmc1* were transformed respectively into multilocular mutant *Bjmc1* which showed four valves per silique (Fig. 4c). A total of 56 *Bjmc1*-transgenic plants and 32 *Bjmc1*-transgenic plants were obtained in T0 generation. 33 out of the 56 *Bjmc1*-transgenic plants showed chimeric phenotype, while 17 out of the 32 *Bjmc1*-transgenic plants showed completely bilocular phenotype (Fig. 3b,c). Further analysis of phenotypes and genotypes confirmed that the transgenic events were cosegregated with the bilocular trait in T1 progeny.

***Bjmc1* encoded a putative truncated protein.** Semi-quantitative reverse transcription polymerase chain reaction (RT-PCR) was performed to analyze the transcription levels of *Bjmc1* and *Bjmc1* of early in o-rescences of bilocular and trilocular plants in BC₅F₁ generation. C1-2 and M1-1 (Supplementary Table 1) were designed according to different parts of the gene sequence (Fig. 2a). Both C1-2 and M1-1 could identify the transcription of *Bjmc1* in bilocular plants, while only C1-2 could identify the transcription of *Bjmc1* in trilocular plants, indicating that the truncation of transcription has occurred in *Bjmc1* gene. Although the transcription of *Bjmc1* and *Bjmc1* could be detected by C1-2, the expression was down-regulated in trilocular plants (Supplementary Fig. 1i).

To investigate the transcription level of *Bjmc1* and *Bjmc1* in detail, the full-length complementary DNAs (cDNAs) were identified by RACE technology. The cDNA of *Bjmc1* was 3,155 bp in length, which was composed of two exons and consists of a 71 bp 5' untranslated region, a 2,964 bp ORF and a 136 bp 3' untranslated region. The cDNA of *Bjmc1*, with a full-length of 2,583 bp, comprised a 71 bp 5' untranslated region which contained the same sequence with the cDNA of *Bjmc1*, a 2,349 bp ORF and a 159 bp 3' untranslated region (Fig. 2b and Supplementary Data 4). *Bjmc1* encoded a putative protein of 987 amino acids and contained two putative transmembrane domains, a putative extracellular domain consisting of 6 complete Leu-rich repeats (LRRs) and a putative intracellular domain containing all of the conserved residues found in serine/threonine protein kinase.

The LRR region was flanked by a pair of conservatively spaced cysteines (Fig. 2a,b). Sequence analysis indicated that the putative protein consisting of 782 amino acids contained the extracellular domain of *RLK1*, and further analysis showed that this protein was derived from the truncation of *RLK1* gene at Gly⁷⁸² by Copia-LTR RTE1 (Fig. 2b and Supplementary Fig. 3c), proving that the serine/threonine protein kinase domain of *RLK1* gene was required for the gene to control the development of siliques in *B. juncea*.

The dominant negative effect of *Bjmc1*. In back-cross populations, we observed that some bilocular individuals (*Bjmc1*^{+/+}) showed several trilocus-like siliques which showed trilocular shape but with two locules and only a few siliques had three locules (Fig. 4a,b). The silique trait of 219 bilocular plants was investigated in BC₈F₁ generation, and 92 individuals were found to have trilocus-like siliques.

A previous report has demonstrated that all intermediate and strong *Bjmc1* alleles in *B. juncea* are dominant negative²⁷. Similar to the homozygous mutant of *RLK1* homologous gene, the heterozygous plants also exhibited weak fasciation in tomato¹⁶. Moreover, the *RLK1*, a Leu-rich repeat receptor-like Ser/Thr kinase, regulated organ shape and inflorescence architecture, and a truncated *RLK1* protein that lacks the cytoplasmic kinase domain confers dominant-negative effects³⁰. In our research, *Bjmc1* was shown to be able to encode a truncated protein with a similar structure with *RLK1* protein, indicating the possibility of dominant negative effect. To verify whether *Bjmc1* protein functions in the development process of carpel, the construct *Bjmc1*::*RLK1* was transformed into *B. juncea* mutant. A total of 62 transgenic plants were obtained and 25 of them showed siliques with five valves (Fig. 4c). The phenotype analysis of T₁ progeny showed that the transgenic events could be cosegregated with the phenotype of five valves. The over-expression of *Bjmc1* could aggravate the multilocular phenotype of *B. juncea*. These results further supported the inference that the truncated *Bjmc1* protein showed the dominant negative character in controlling carpel development.

Expression pattern and subcellular localization of *BjMc1*.

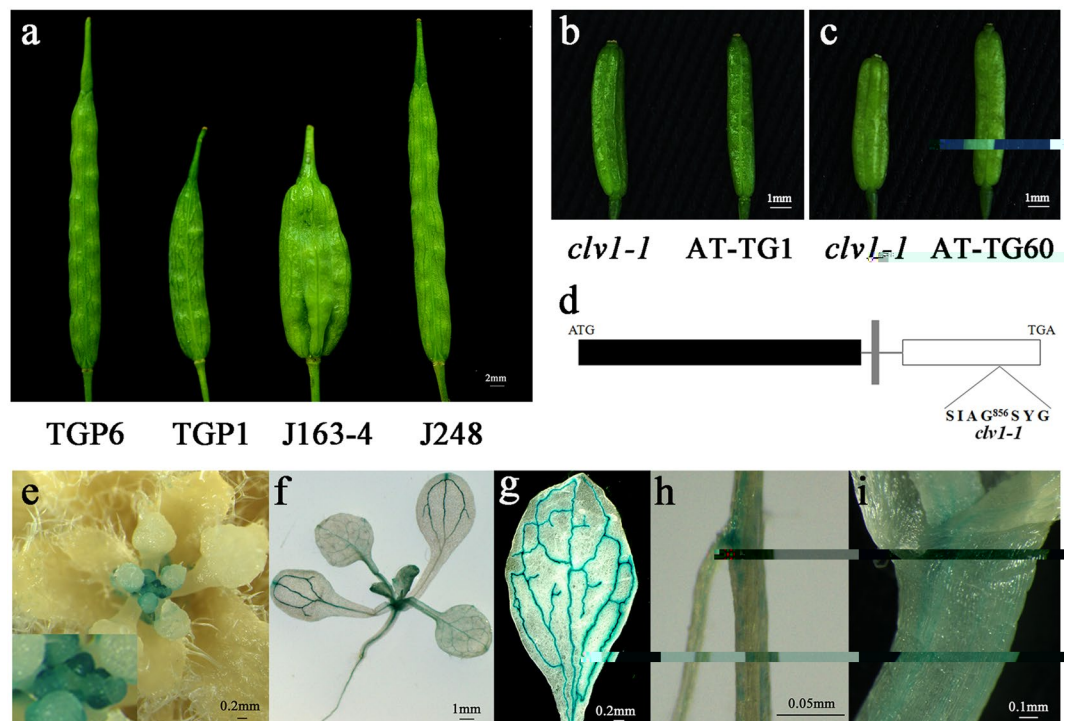


Fig. 3. Functional analysis and expression pattern of transgenic lines. (a) Silique phenotypes of transgenic T₀ line TGP6, TGP1, J163-4 and bilocular parental J248. (b) Silique phenotypes of transgenic T₀ line TGP1, multilocular parental J163-4 mutant and bilocular parental J248. (c) Silique phenotypes of transgenic T₀ line AT-TG1. (d) Schematic of the mutation sites of *clvl-1*. (e–i) Representative histochemical analysis of GUS expression in tissues under the control of the *clvl-1* promoter in the transgenic T₂ plants. (e) Early inflorescence with lower bud meristems. (f) Seedling 10 days after germination. (g) Rosette leaf. (h) Root. (i) Stem.

To investigate the subcellular localization of *clvl-1*, we fused the coding region containing putative transmembrane domains and LRR domains, a without serine/threonine protein kinase of *clvl-1* with the coding region of an enhanced GFP driven by a double 35S promoter. This chimeric plasmid was transformed into *N. glauca*. The result showed that the GFP fusion protein was localized in the plasma membrane (Supplementary Fig. 1c–h), which was consistent with the previous study³¹ and suggested that *clvl-1* could retain some conserved functions of its homologs in other species.

Expression analysis of genes involved in early inflorescence. According to the expression pattern of *clvl-1* gene, the homologous genes of *clvl-1* signaling pathway, including *clvl-1*, *clvl-2*, and *clvl-3*, and the homologous genes of ABC model of floral organ identity, including *clvl-1*, *clvl-2*, and *clvl-3*, were chosen to perform the qPCR analysis using the total RNA extracted from the early inflorescence of bilocular and trilobular plants in BC₅F₁ generation, and primers (Supplementary Table 1) were design according to these homologous gene sequences. The results showed that, in trilobular plants, the A class genes, *clvl-1* and *clvl-2*, were down-regulated significantly, the B class genes, *clvl-3* and *clvl-4* were up-regulated significantly, and the C class gene, *clvl-5*, was also down-regulated significantly (Fig. 5). In trilobular plants, the signaling pathway genes, *clvl-1* and *clvl-2*, were down-regulated significantly, and *clvl-3* was up-regulated. However, as two key components of signaling pathway, *clvl-1* and *clvl-2* did not show significant variations between bilocular and trilobular plants in early inflorescence (Fig. 5). These results indicated that *clvl-1* gene participated in signaling pathway, but it was not the key pathway to control the carpel development in *N. glauca*. The mutant of *clvl-1* gene in trilobular plants resulted in the significant expression variation of ABC class genes, indicating that *clvl-1* involved in the pathway of lower bud formation to control the carpel development.

Mc1 genes being conserved and widespread in land plants. Blast searching against the plant database revealed that *clvl-1* genes were widespread in land plants and each sequenced land plant genome contained at least one gene encoding *clvl-1* homologue. To explore the evolutionary process of *clvl-1* in land plants, we characterized CDSs and proteins of *clvl-1* genes from species representing the main lineages of land plants, including moss, lycopphyte, Amborellaceae, 9 monocot species and 24 dicot species. These genes could be divided into three major branches on the phylogenetic tree (Supplementary Fig. 4), and *clvl-1* was in the branch of the Cruciferae species. Structural analysis of *clvl-1* genes



Fig e 4. Dominant negative phenotype. (a) Silique phenotype of the bilocular plant in BC₅F₁ generation. (b) Bilocular silique, trilocular silique and trilocular-like silique. (c) Silique phenotypes of Arabidopsis mutant and -transgenic T0 line AT-TG100.

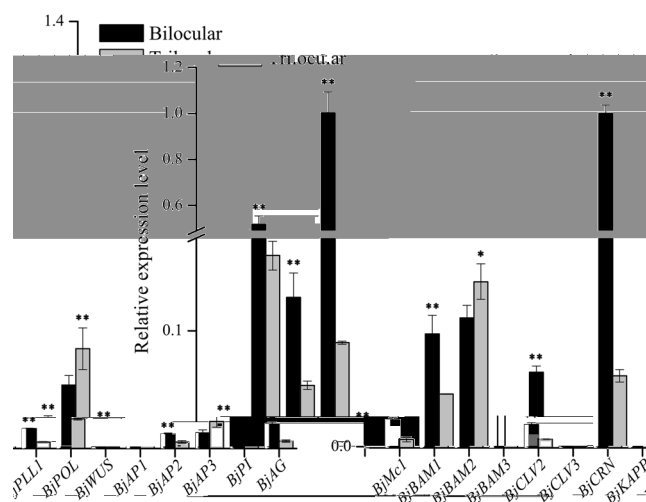


Fig e 5. e difference of expression level of related genes between bilocular and trilocular plants during the lower bud differentiation period in BC₅F₁ generation. *P < 0.05; **P < 0.01

in land plants was performed by comparing the exon-intron organization (<http://gsds.cbi.pku.edu.cn/>). It was shown that the coding regions of all genes of land plants were interrupted by 1–2 introns except for , which contained 8 introns and 9 exons (Supplementary Fig. 5).

Two amino acid sites underwent positive selection in the ancestors of *Mc1* genes. In this research, we attempted to further reveal the evolutionary process of homologous genes in land plant species. The LRT of positive selection was applied using method and the codon substitution models^{32–34}, and all genes of sampled land plants were tested respectively. First, one-ratio model was used to determine whether there were variations in : ratio of the codon position for genes in land plants. Overall, the maximum likelihood estimates for : values were close to zero (Supplementary Table 3), suggesting that purifying selection was the predominant force in the evolution of in land plants. Second, the LRTs to compare the data t to models M1a vs M2a and M7 vs M8 were used to determine whether positive selection promoted the divergence of genes in land plants. No amino acid site was influenced by positive selection during the evolution of genes in land plants. These results indicated that the primary constraint for genes in land plants was purifying selection.

To assess whether the ancestors of gene had undergone a pattern of molecular evolution in the evolutionary process of land plants, branch-model of was performed. Six branches were selected from the phylogenetic tree (branch I, II, III, IV, V and VI) (Supplementary Fig. 4). We found that for branch I and II, the branch-model permitting a class of positively selected codons with : > 1 had a significantly better fit to the data than the branch-model in which this class of codons were restricted to : = 1. However, this was not the case for branch III, IV, V and VI (Supplementary Table 4). The results indicated that the evolution process of gene might be influenced by positive selection in its ancestors of branch I and II. Because LRTs suggested that positive selection acted on the ancestral species of gene, the method of Bayes empirical Bayes³⁴, namely branch-site-model of , was used to evaluate the positively selected sites and their posterior probabilities. A total of 32 codons were identified with a >50% posterior probability of : > 1 along branch I. Of these codons, 2 amino acid sites had a >95% posterior probability of positive selection. Although 2 and 6 codons were identified with a >50% posterior probability of : > 1 along branch III and branch IV respectively, no amino acid site had a posterior probability ≥95% of positive selection (Supplementary Table 5 and Supplementary Fig. 6). The two positive sites of branch I were located in the first cysteine domain and a key component of serine/threonine protein kinase domain respectively. When dicots and monocots were diverged from Moss, Lycophyte and Amborellaceae, the 139th amino acid tryptophan (W) located in the first cysteine domain was mutated into phenylalanine (F), and the 899th amino acid cysteine (C) located in a component of serine/threonine protein kinase domain was mutated into valine (V) except for in , and (Supplementary Fig. 2 o

multiloculus had variable valve numbers in the siliques of the same plant^{10, 11}. However, in this study, J163-4 planted in both central and northwestern China exhibited four valves stably in trilocular siliques. We transformed the gene into the allele in for over-expression, and proved that the truncated protein had a potential dominant negative effect, which could have played a key role in maintaining the

a Genotype: *BiMc1BiMc1*

b Genotype: *BiMc1Bimc1*

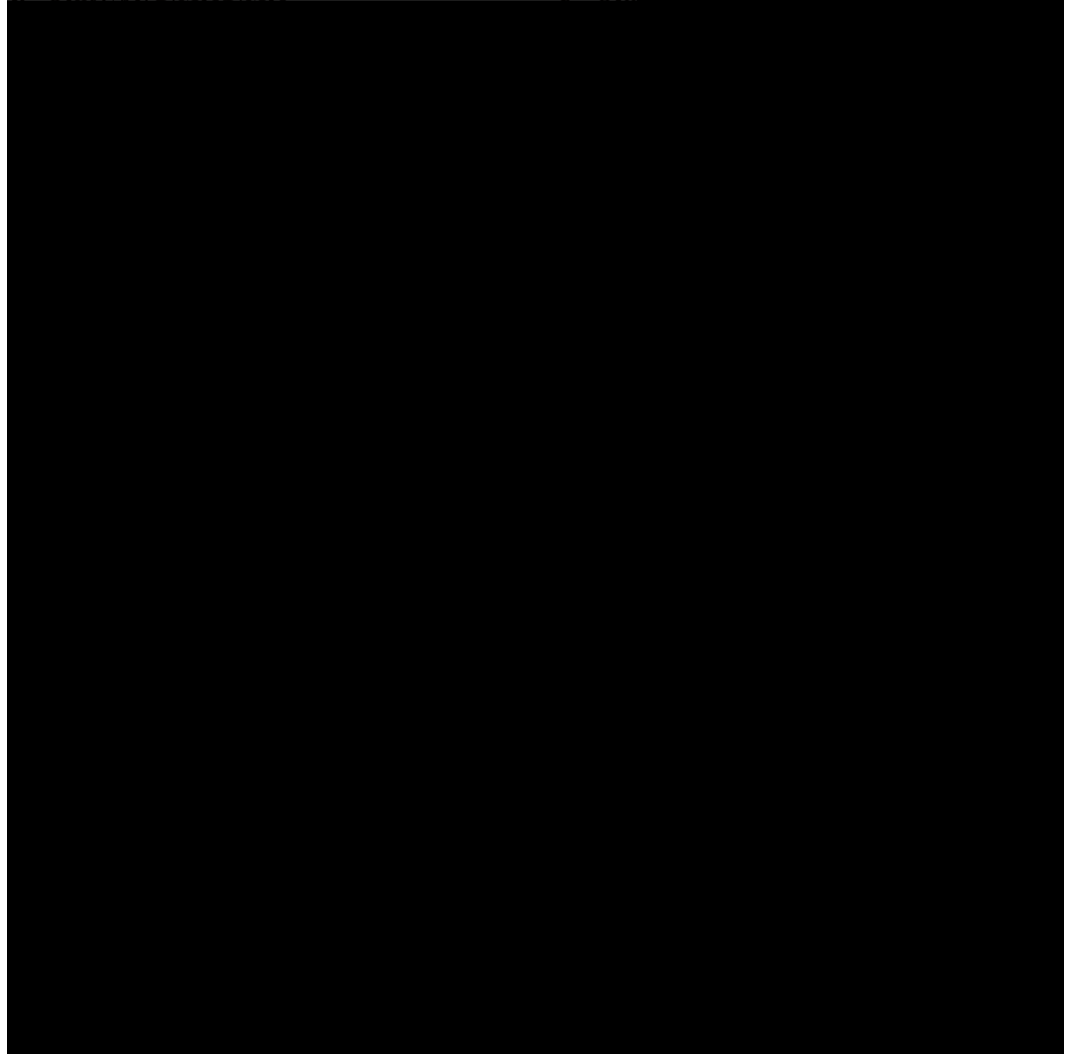


Fig 6. Model of dominant negative receptor action in *Arabidopsis*. A putative model for the role of protein, *BiMc1* () protein and the ligand protein in regulating the carpel development. Bold arrows indicate that the *BiMc1* protein plays a dominant role in regulating the development of carpel. (a) Scenarios for plants with genotype of *BiMc1BiMc1*. The ligand could bind to both the *BiMc1* and *BiMc1* protein, but *BiMc1* protein was the dominant receptor kinase. (b) Scenarios for plants with genotype of *BiMc1Bimc1*. The ligand could bind to the *BiMc1*, *Bimc1* and *BiMc1* protein, and the *BiMc1* protein was the dominant receptor kinase. (c) Scenarios for plants with genotype of *BiMc1BiMc1*. The ligand could bind to the *BiMc1* and *BiMc1* protein, but only the *BiMc1* protein which does not play the dominant role in regulating pathway has the normal function. (d) Scenarios for plants with genotype of *BiMc1BiMc1* and overexpression. More ligands are possessed by the *BiMc1*, and little ligand could bind to the *BiMc1* protein.

Availability of data and material. All data generated or analyzed during this study are included in this published article and its additional files.

BAC screening and sequencing. Positive clones from the purple-leaf mustard () bacterial artificial chromosome (BAC) library were identified through a two-stage polymerase chain reaction (PCR) screening method with C1-1 primers designed from the sequence of *BiMc1* which was located near the homologous sequence of molecular marker SC13 in A07 chromosome of *Arabidopsis*. The phenotypes were similar between J163-4 and *BiMc1* mutant in *Arabidopsis* (Crooijmans et al., 2000). BAC DNA was sequenced as previously described by Yi et al. (2000).

Genetic mapping and positional cloning. Bulk segregant analysis⁴¹ was conducted to screen the molecular markers linked to *BiMc1* locus. Simple sequence repeats (SSR) was designed according to the reference sequence retrieved from the positive BAC clone. The parents and bulks were subjected to SSR marker analysis. PCR was performed according to Xu et al. (2000). PCR products were then separated on 1% polyacrylamide denaturing

sequencing gel and shown by silver nitrate staining. Linkage analysis was performed using Joinmap4⁴². All genetic distances were expressed in centiMorgan (cM) using the Kosambi function⁴³.

cDNA preparation and 5'- and 3'- rapid-amplification of cDNA ends (RACE). Total RNA was extracted from various plant tissues using an RNA extraction kit (RNeasy Plant Mini Kit; QIAGEN). The first-strand cDNA was synthesized using 2 mg of RNA and 200 units of M-MLV reverse transcriptase (Promega Kit) in a volume of 25 µl. The 5'- and 3'- RACE reactions were performed using the SMARTer RACE Amplification Kit (Clontech) according to manufacturer's instructions.

Constructs and transformation. The genomic fragments of the candidate gene were amplified from the bilocular plants from the NILs using high-fidelity PCR. A 6,613 bp genomic DNA fragment spanning from 2,692 bp upstream the translation start codon to 767 bp downstream the termination codon of the gene was amplified using primer E48-2 (Supplementary Table 1) as forward primer. The correct fragment confirmed by sequencing was then cloned into Pst I - Kpn I site of pCambia2300 vector to construct plasmid pE48-2. To prepare the Pro_{BjMc1}-GUS construct, we cloned a 3,455 bp genomic DNA fragment spanning from start codon to 301 bp downstream the termination codon of the gene using primer E46-1 (Supplementary Table 1) into Pst I - Kpn I site of pCambia2300, and double 35S promoter was cloned into Hind III - Pst I site of pCambia2300. To prepare the Pro_{BjMc1}-GUS construct, the promoter region (from 1 to 2,499 bp) using primer E58-1 (Supplementary Table 1) was amplified. A cassette containing GUS coding region followed by nopaline synthase polyadenylation signal from pBI101 vector was subcloned into the binary vector pCambia 2300 with restriction enzymes Hind III and EcoR I to construct promoter-GUS fusions. The amplified fragments were subcloned into the modified binary vector pCambia 2300 to yield the 2,499 bp promoter-GUS construct. To prepare the Pro_{BjMc1}-GUS construct, a 3,036 bp genomic DNA fragment spanning from the start codon to a 687 bp downstream DNA fragment using primer HY-4 (Supplementary Table 1) was amplified. The correct fragment confirmed by sequencing was cloned into Xba I - Sac I site of pMDC83 vector to construct plasmid pHY-4. These constructs were introduced into the host cells of Agrobacterium strain GV3101. The Pro_{BjMc1}-GUS and Pro_{BjMc1}-GUS constructs were transformed into the trilocular line J163-4, whereas Pro_{BjMc1}-GUS construct was introduced into wild-type (ecotype) and Pro_{BjMc1}-GUS was transformed into Pro_{BjMc1}-GUS by oral dipping⁴⁴. The T₂ transgenic plants of Pro_{BjMc1}-GUS were grown for GUS staining.

Expression analysis. Total RNA was extracted using Trizol reagent (Invitrogen). The tissues of the early in-orecence of trilocular plants and SAM, early in-orecence, 1–4 mm ovary, 4–7 mm ovary, 7–10 mm ovary, silique peel, leaves, stem and root of bilocular plants in BC₃F₁ generation were selected, and 3 mg of total RNA from each tissue was treated with RNase-free DNase I to remove contaminated DNA respectively, then reverse transcribed into the first-strand complementary DNA (cDNA) with M-MLV reverse transcriptase (Fermentas, Vilnius, Lithuania) using oligo d(T)₂₅ primer. The reverse-transcribed products from various tissues were used as templates for qPCR assay using the Bj3 primer (Supplementary Table 1) which could particularly amplify copy to examine the expression of the gene. The qPCR was conducted according to Li⁴⁴. The measurements were obtained using the relative quantification method⁴⁵. The gene was used as the internal control for⁴⁶. All expression level data obtained by qPCR were based on three biological samples and three replicates for each sample.

The cDNA of the gene and the gene were detected from the reverse-transcribed products from early in-orecence of trilocular and bilocular plants in BC₃F₁ generation using the semi-quantitative RT-PCR by C1-2 and M1-1. The gene was used as the control. Semi-quantitative RT-PCR was performed as following: 94 °C for 3 min; twenty-five cycles of 94 °C for 30 s, 55 °C for 30 s and 72 °C for 45 s; and a final 10-min elongation step.

Histochemical GUS staining. Twelve independent T₂ transgenic lines of Pro_{BjMc1}-GUS were subjected to histochemical GUS assays. Seedlings of 10 d and various organs of the transgenic plants were incubated at 37 °C overnight in 5-bromo-4-chloro-3-indolyl-β-glucuronic acid solution and then cleaned in 75% (v/v) ethanol. The treated tissues were observed on an Olympus IX-70 Microscope equipped with Nomarski Optics⁴.

Subcellular localization of BjMc1. The coding sequence without the termination codon (TAA) was amplified from the bilocular plants in BC₃F₁ generation by PCR using YXB4 primer (Supplementary Table 1). The amplified cDNA fragments were inserted downstream of the double 35S promoter through Xba I - BamH I site in frame with GFP in pMDC83 vector. This plasmid was transformed into Agrobacterium strain GV3101. The roots of transgenic plants in T₂ generation were incubated with 10 µM FM4-64 for at least 5 min before observation. The emission light was dispersed and recorded at 500–540 nm for GFP. Confocal images were taken with a Nikon Eclipse80i fluorescence microscope equipped a water-immersed ×40 lens with an excitation wavelength of 488 nm and the following detection wavelengths: 500–540 nm for GFP and at >650 nm for FM4-64 (Nikon, Japan). All fluorescence experiments were independently repeated at least three times.

Identification of Mc1 genes from Cruciferae and other land plant species. To identify homologous genes in Cruciferae, BLAST analysis using protein sequence of the gene as a query was performed in Cruciferae (<http://brassicadb.org/brad/>, <http://www.arabidopsis.org/>, <http://122.205.95.67/blast/blast.php>).

To identify homologous genes in the land plants, the coding sequence (CDS) of the gene was used as query to search the National Center for Biotechnology Information (<http://www.ncbi.nlm.nih.gov/>), Ensembl Plants (<http://plants.ensembl.org/index.html>) and the Arabidopsis Information Resource database (<http://www.arabidopsis.org/>). The most highly similar sequence was selected from each species. The deduced nucleotide and protein sequences of land plant genes identified in this analysis were used for further analysis.

Phylogenetic analyses and detection of positive selection. Using the MEGA5⁴⁷, Cruciferae amino acid sequences were aligned by ClastalW and land plant CDSs were aligned by ClastalW condons, and finally the FASTA formats were exported. The maximum-likelihood approach was used for the phylogenetic analysis of Cruciferae and all the land plants, respectively.

To test the selective pressure of genes during the long period of evolution in land plants, the value of ω ratio (or dN/dS) for genes was calculated with the program from Phylogenetic Analysis by Maximum Likelihood (PAML) v4.4³². In this study, three likelihood ratio tests (LRTs), M0, M1a vs M2a and M7 vs M8, were used to examine the selective pressure. M0 was used to calculate the average value of all codon sites, and the other two LRTs were used to detect the role of positive selection. For one LRT, the differences of log likelihood of the two models were compared using chi-squared (χ^2) statistics. In our analyses, the degree of freedom was 1 for M1a/M2a and M7/M8 tests^{33, 48}.

The improved branch model and branch site model⁴⁹ were also used to detect the role of positive selection on the land plant genes. In these two models, six branches were selected from the phylogenetic tree (branch I, II, III, IV, V and VI); and when any one of the branches served as the foreground branch, the remaining branches were background branches (Supplementary Fig. 4). For the analysis of branch site model, we compared the null hypothesis (fixed to 1) with the alternative hypothesis (free) to test whether positive selection affected the evolution of land plant genes. The Bayes empirical Bayes procedure in³⁴ was used to calculate the posterior probability that each site in the foreground branch was subjected to positive selection.

References

- Barton, M. K. Twenty years on: the inner workings of the shoot apical meristem, a developmental dynamo. *Development* 131, 95–113 (2010).
- Li, Z. W. Primary study on anatomic and genetic analyses of multi-loculus in *Brassica napus*. *Acta Horticulturae Sinica* 34, 461–466 (2012).
- He, Y. T. Anatomic and genetic studies on multicapsular character in *Brassica napus* L. *Acta Horticulturae Sinica* 25, 1–4 (2003).
- Li, S. P. Functions as a positive regulator of the number of seeds per silique in *Brassica napus* by regulating the formation of functional female gametophytes. *Plant Cell* 169, 2744–2760 (2015).
- Liu, J. Natural variation in *Brassica napus* gene simultaneously affects seed weight and silique length in polyploid rapeseed. *Plant Cell* 112, 5123–5132 (2015).
- Zhang, L. W., Li, S. P., Chen, L. & Yang, G. S. Identification and mapping of a major dominant quantitative trait locus controlling seeds per silique as a single Mendelian factor in *Brassica napus* L. *Plant Cell* 125, 695–705 (2012).
- Zhao, H. C. Performances in main characteristic of multilocular *Brassica napus*. *Acta Horticulturae Sinica* 12, 62–64 (2003).
- Choudhary, B. R. & Solanki, Z. S. Inheritance of silique locule number and seed coat colour in *Brassica napus*. *Acta Horticulturae Sinica* 126, 104–106 (2007).
- Yadava, S. K. Tetralocular ovary and high silique width in yellow sarson lines of *Brassica napus* (subspecies trilocularis) are due to a mutation in *Brn1* gene, a homologue of *Brn1* in *Arabidopsis thaliana*. *Plant Cell* 127, 2359–2369 (2014).
- Xiao, L. Genetic and physical fine mapping of a multilocular gene in *Brassica napus* to a 208-kb region. *Plant Cell* 32, 373–383 (2013).
- Fan, C. C. A novel single-nucleotide mutation in a *Brn1* gene homologue controls a multilocular silique trait in *Brassica napus* L. *Plant Cell* 7, 1788–1792 (2014).
- Clark, S. E., Running, M. P. & Meyerowitz, E. M. *Brn1*, a regulator of meristem and flower development in *Arabidopsis thaliana*. *Development* 119, 397–418 (1993).
- Muller, R., Bleckmann, A. & Simon, R. The receptor kinase *Brn1* of *Arabidopsis thaliana* transmits the stem cell-limiting signal independently of *Brn1*. *Plant Cell* 20, 934–946 (2008).
- Forstheofel, N. R., Wu, Y., Schulz, B., Bennett, M. J. & Feldmann, K. T-DNA insertion mutagenesis in *Arabidopsis thaliana*: prospects and perspectives. *Plant Cell* 10, 353–366 (1992).
- Kayes, J. M. & Clark, S. E. *Brn1*, a regulator of meristem and organ development in *Arabidopsis thaliana*. *Development* 125, 3843–3851 (1998).
- Xu, C. A cascade of arabinosyltransferases controls shoot meristem size in tomato. *Plant Cell* 47, 784–792 (2015).
- Durbak, A. D. & Tax, F. E. Signaling pathway receptors of *Arabidopsis thaliana* regulate cell proliferation in fruit organ formation as well as in meristems. *Plant Cell* 189, 177–194 (2011).
- Cheng, Z. P., Yang, Z. N. & Zhang, S. *Brn1* interacts with *Brn1* in modulation of gynoecium development in *Brassica napus*. *Plant Cell* 56, 13–23 (2013).
- Prunet, N. *Brn1* promotes stem cell homeostasis and floral meristem termination in *Arabidopsis thaliana* through *Brn1* and *Brn1* signaling. *Plant Cell* 66, 6905–6916 (2015).
- Mandel, T. The *Brn1* receptor kinase regulates *Arabidopsis thaliana* shoot apical meristem size, phyllotaxy and floral meristem identity. *Plant Cell* 141, 830–841 (2014).
- Bommert, P. *Brn1* encodes a putative maize ortholog of the *Brn1* leucine-rich repeat receptor-like kinase. *Plant Cell* 132, 1235–1245 (2004).
- Bommert, P., Nagasawa, N. S. & Jackson, D. Quantitative variation in maize kernel row number is controlled by the *Brn1* locus. *Plant Cell* 45, 334–337 (2013).
- Suzaki, T. The *Brn1* gene regulates floral meristem size in rice and encodes a leucine-rich repeat receptor kinase orthologous to *Brn1*. *Plant Cell* 131, 5649–5657 (2004).
- Medford, J. I., Behringer, F. J., Callos, J. D. & Feldmann, K. A. Normal and abnormal development in the *Arabidopsis thaliana* vegetative shoot apex. *Plant Cell* 4, 631–643 (1992).
- Pogany, J. A. Identifying novel regulators of shoot meristem development. *Plant Cell* 111, 307–313 (1998).
- Clark, S. E., Williams, R. W. & Meyerowitz, E. M. The *Brn1* gene encodes a putative receptor kinase that controls shoot and floral meristem size in *Arabidopsis thaliana*. *Development* 89, 575–585 (1997).
- Diévert, A. Dominant-negative alleles reveal functional overlap between multiple receptor kinases that regulate meristem and organ development. *Plant Cell* 15, 1198–1211 (2003).
- Xu, P. Identification of molecular markers linked to trilocular gene (*Brn1*) in *Brassica napus* L. *Plant Cell* 33, 425–434 (2014).
- Wang, G. Fine mapping of polycyclic gene (*Brn1*) in *Brassica napus* L. *Plant Cell* 42, 1735–1742 (2016).
- Shpak, E. D., Lakeman, M. B. & Torii, K. U. Dominant-Negative Receptor Uncovers Redundancy in the Leucine-Rich Repeat Receptor-Like Kinase Signaling Pathway at Regulates Organ Shape. *Plant Cell* 15, 1095–1110 (2003).
- Stahl, Y. Moderation of root stemness by *Brn1* and *Brn1* receptor kinase complexes. *Plant Cell* 23, 362–371 (2013).

32. Yang, Z. PAML 4: phylogenetic analysis by maximum likelihood. *Molecular Biology and Evolution* **24**, 1586–1591 (2007).
33. Nielsen, R. & Yang, Z. Likelihood models for detecting positively selected amino acid sites and applications to the HIV-1 envelope gene. *Molecular Biology and Evolution* **148**, 929–936 (1998).
34. Yang, Z., Wong, W. S. & Nielsen, R. Bayes empirical bayes inference of amino acid sites under positive selection. *Molecular Biology and Evolution* **22**, 1107–1118 (2005).
35. Yang, J. H. The genome sequence of allopolyploid *Arabidopsis thaliana* and analysis of differential homeolog gene expression in *Arabidopsis thaliana* selection. *Genome Biology* **48**, 1225–1232 (2016).
36. Herskowitz, I. Functional inactivation of genes by dominant negative mutation. *Cell* **329**, 219–222 (1987).
37. DeYoung, B. J. The *Arabidopsis thaliana* *ERF1*-related *ERF2*, *ERF3*, and *ERF4* receptor kinase-like proteins are required for meristem function in *Arabidopsis thaliana*. *Plant Cell* **45**, 1–16 (2006).
38. Ping, J. Q. *AtGUS1* is a gain-of-function MADS-domain factor gene that specifies semideterminacy in soybean. *Plant Cell* **26**, 2831–2842 (2014).
39. Nagaharu, U. Genome analysis in *Arabidopsis thaliana* with special reference to then experimental formation of *Arabidopsis thaliana* and peculiar mode of fertilization. *Genetics* **7**, 389–452 (1935).
40. Yi, B. Two duplicate CYP704B1 homologous genes *CYP704B1A* and *CYP704B1B* are required for pollen exine formation and tapetal development in *Arabidopsis thaliana*. *Plant Cell* **63**, 925–938 (2010).
41. Michelmore, R. W., Paran, I. & Kesseli, R. Identification of markers linked to disease-resistance genes by bulked segregant analysis: a rapid method to detect markers in specific genomic regions by using segregating populations. *Molecular Breeding* **88**, 9828–9832 (1991).
42. van Ooijen, J. Joinmap® software for the calculation of genetic linkage maps in experimental populations, version 4. Wageningen, the Netherlands: Kyazma BV (2006).
43. Kosambi, D. The estimation of map distances from recombination values. *Genetics* **12**, 172–175 (1943).
44. Clough, S. J. & Bent, A. F. Floral dip: a simplified method for *Agrobacterium*-mediated transformation of *Arabidopsis thaliana*. *Nature Biotechnology* **16**, 735–743 (1998).
45. Livak, K. J. & Schmittgen, T. D. Analysis of relative gene expression data using real-time quantitative PCR and the $2^{-\Delta\Delta CT}$ Method. *Methods* **25**, 402–408 (2001).
46. Ameilhe, A. K., Eve, S., Stephen, J. P., Smita, K. & Peter, J. E. Suppression of the *AtGLG1* triacylglycerolipase family during seed development enhances oil yield in oilseed rape (*Brassica napus*). *Plant Cell* **11**, 355–361 (2013).
47. Tamura, K. MEGA5: molecular evolutionary genetics analysis using maximum likelihood, evolutionary distance, and